数理解析研究所講究録
第1614巻 2008年 166-171

Applications of computational homology to 3D morphology transitions
計算ホモロジーの複雑な空間パターンへの応用

千歳科学技術大学　寺本 敬 (Takashi Teramoto)
CHITOSE INSTITUTE OF SCIENCE AND TECHNOLOGY

北海道大学・電子科学研究所　マルシオ ガメイロ (Marcio Gameiro)
RESEARCH INSTITUTE FOR ELECTRONIC SCIENCE, HOKKAIDO UNIVERSITY

北海道大学・電子科学研究所　西浦廉政 (Yasumasa Nishiura)
RESEARCH INSTITUTE FOR ELECTRONIC SCIENCE, HOKKAIDO UNIVERSITY

It is well established both experimentally and numerically that nonlinear systems can generate complex spatio-temporal patterns. Characterizing the geometry of these complex patterns quantitatively is a long-standing challenge. Algebraic Topology, and in particular Homology, is a classical mathematical tool for the global analysis of nonlinear spaces and functions [4], which provides very basic topological (geometrical) information about the patterns, such as the number of components (pieces) and the number of holes. For three-dimensional morphologies it also provides the number of voids. Computationally efficient algorithms and software for the homology computation are developed in the Computational Homology Project (the software package can be downloaded from the CHomP website [1]) and they allow us to compute homology of cubical sets and maps, i.e., complex structures obtained from experimental observation and numerical simulations can be quantified by using a coherent set of mathematical techniques [2].

In our previous papers [6, 7], we investigated the geometric measures, surface area $S(\Gamma)$ and curvature of the level set Γ for the three-dimensional morphologies obtained as minimizers in diblock copolymer problem and demonstrate the mechanism behind the appearance of the double gyroid morphology, i.e., the morphology arising from the incompatibility can be reasonably considered to have been created in order to decrease the interfacial regions. In this way, the diblock copolymer problem can be regarded as the minimization problem, $\min\{F_{\epsilon,\sigma}/\epsilon : |\Omega|^{-1}\int_\Omega u\mathbf{dr} = \overline{u}, \Omega = [0:L)^3\}$, with the free energy functional,

$$F_{\epsilon,\sigma}(u) = \int_\Omega \left(\frac{\epsilon^2}{2}|\nabla u|^2 + W(u) + \frac{\sigma}{2}|(-\triangle)^{-1/2}(u-\overline{u})|^2\right)\mathbf{dr}, \qquad (1)$$

where the notation $\overline{u} = |\Omega|^{-1}\int_\Omega u\mathbf{dr}$ is the space average of the local concentration u [5]. The phenomenological parameters, ϵ and σ, indicate the interface thickness and the strength of the chemical bond, respectively. The double well potential, $W(u) = (u^2-1)^2/4$, in the second term has two minimum values, $u \sim +1$ and -1,

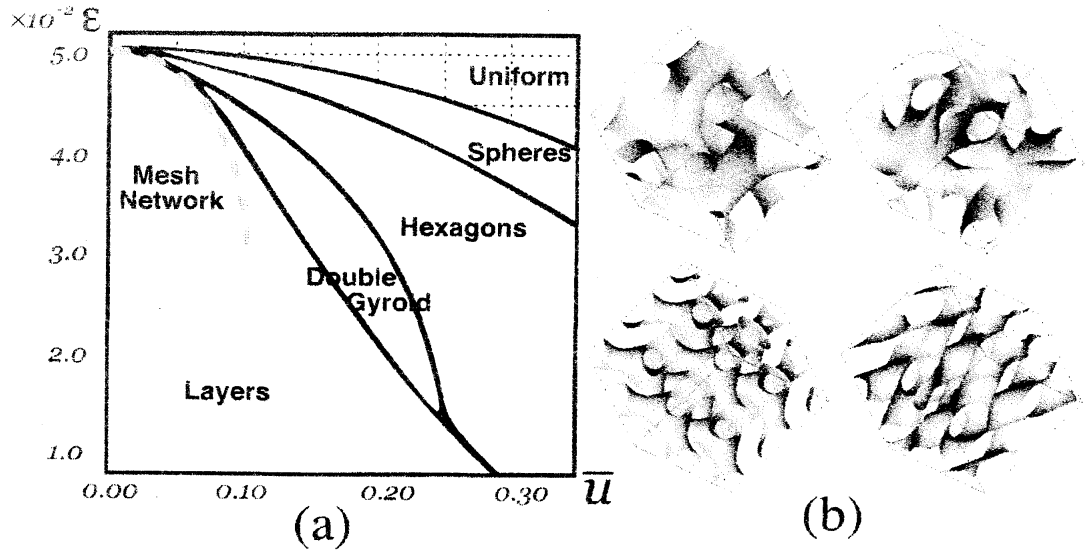

Figure 1: (a) $(\overline{u}, \epsilon)$-phase diagram of global minimizers. On the gray broken curve, mesh network is more stable than double gyroid. (b) Isosurfaces $\Gamma(\overline{u}) \equiv \{\mathbf{r} \in \Omega : u(\mathbf{r}) = \overline{u}\}$ of Double Primitive, Double gyroid, Double Diamond, and Mesh network morphologies from top-left to bottom-right figures.

in relation to two stable states for the local concentration u. Since the first term tries to decrease the interfacial regions and the third term tries to promote formation of the interface, this situation meets the conditions of competition between short-range activation and long-range inhibition. If the system is as described above, even though some details may differ, a mesoscale periodic pattern is expected to appear naturally. The $(\overline{u}, \epsilon)$-phase diagram of global minimizers, with the parameter ratio fixed to $\sigma/\epsilon = 2^{11}(1-\overline{u}^2)^{-2}$, is illustrated in Fig.1(a).

The purpose of this article is to present a new viewpoint for understanding complex dynamics, including morphology transitions, by incorporating topologically invariant quantities, the so-called homological quantities, into the field of materials science, and utilizing them as a means of observation. We measure the topology of a structure by means of its Homology, more specifically, we compute its Betti numbers. For precise definitions and algorithms for computing Homology see [1, 4].

To obtain the data structure needed in the computations, a topological space is decomposed into elementary cubes based on rectangular grids. The variable, $u(\mathbf{r})$, is represented by $\{u(i,j,k)|1 \leq i,j,k \leq N\}$. Now, we determine the Betti number $\{\beta_k(X^{\pm}) = \text{rank } H_k(X^{\pm})|k = 0, \cdots, 3\}$ for the cubical sets $X^- = \{\mathbf{r} \in \Omega|u(\mathbf{r}) < \overline{u}\}$ and $X^+ = \{\mathbf{r} \in \Omega|u(\mathbf{r}) > \overline{u}\}$ divided on the interface $\Gamma(\overline{u})$. The three-dimensional bi-continuous morphologies in Fig.1(b) can be classified in terms of the Betti numbers as depicted in Table 1. Note that they have attracted much interest in the material design for photonic crystals, in which the refractive index changes periodically. Spatial heterogeneity in optical media affects the propagating manner of lights, depending on their wavelength. The Euler characteristic χ can be also

Table 1: The Betti number set and Space group symmetry for the Primitive, Gyroid, Diamond, and Mesh network morphologies appear in diblock copolymer problems.

	single network			double network		
	$\beta_i(X^-)$	$\beta_i(X^+)$	symmetry	$\beta_i(X^-)$	$\beta_i(X^+)$	symmetry
P	(1, 3, 0, 0)	(1, 3, 0, 0)	$Pm\bar{3}m$	(2, 6, 0, 0)	(1, 6, 1, 0)	$Im\bar{3}m$
G	(1, 5, 0, 0)	(1, 5, 0, 0)	$I4_132$	(2, 10, 0, 0)	(1, 10, 1, 0)	$Ia\bar{3}d$
D	(1, 9, 0, 0)	(1, 9, 0, 0)	$Fd\bar{3}m$	(2, 18, 0, 0)	(1, 18, 1, 0)	$Pn\bar{3}m$
M	(1, 13, 0, 0)	(1, 13, 0, 0)	Fddd			

used to infer geometric properties, specifically the Gauss curvature via the Gauss-Bonnet Theorem. Notice that the Betti numbers provide more detailed topological information than $\chi = \sum_{k=0}^{3}(-1)^k\beta_k$.

Next, we perform by numerical simulations of the morphology transition dynamics seen in a weak separation region based on the created phase diagram. We use an evolution equation of a gradient system that ensures the Lyapunov function $F_{\epsilon,\sigma}$ will monotonically decrease over time while conserving the average $\overline{u}$:

$$\begin{aligned} \frac{\partial u}{\partial t} &= \Delta\left(\frac{\delta F_{\epsilon,\sigma}}{\delta u}\right), \\ &= \Delta\{-\epsilon^2\Delta u - u + u^3\} - \sigma(u - \overline{u}). \end{aligned} \tag{2}$$

As a first step, we check the transition from unstable hexagons to stable spheres at parameters $(\overline{u}, \epsilon) = (0.30, 4.0\times10^{-2})$. When doing this, we fix the cell side length, $L \simeq 1.17$, that numerically gives the global minimizers at the phase boundary between hexagons and spheres. As shown in Fig.2(b), the number of hexagonal cylinder domains is $\beta_0(X_{\rm H}^-) = 4$, while that of bubbles is $\beta_0(X_{\rm S}^-) = 16$. For the topological identification of morphology transitions, it is more natural to consider the homology group of $X_{\rm H}^-$ relative to $X_{\rm S}^-$. The relative homology $H_k(X_{\rm H}^-, X_{\rm S}^-)$ is equal to the regular homology of the quotient space $X_{\rm H}^-/X_{\rm S}^-$, i.e., the topology of $X_{\rm H}^-$ modulo $X_{\rm S}^-$. This homology $H_k(X_{\rm H}^-, X_{\rm S}^-)$ measures pipes detected by chain complexes whose boundaries lie in $X_{\rm S}^-$ [4]. In this manner, the first relative Betti number, i.e., rank of $H_1(X_{\rm H}^-, X_{\rm S}^-)$, is obtained as $\beta_1(X_{\rm H}^-, X_{\rm S}^-) = 16$. This result confirms that four hexagonal cylinder domains were destabilized to form narrow necks in their axial directions, and they were divided into 16 spherical domains.

Next, we check the transition from layers to hexagons at the parameters $(\overline{u}, \epsilon) = (0.20, 4.0 \times 10^{-2})$. Unlike the above case of a columnar domain fragmenting into spherical domains, as shown in Figs.2(c)(d), a perforated layers morphology of $\beta_i(X_{\rm PL}^-) = (2, 18, 0, 0)$ appears as an intermediate state during morphology transition, i.e., this transition proceed in two stages: the first is that from layers to perforated layers and the second is that from perforated layers to hexagons. The second relative Betti numbers for the first transition is computed as $\beta_2(X_{\rm L}^-, X_{\rm PL}^-) = 16$ and the first relative Betti numbers for the second transition is computed as $\beta_1(X_{\rm PL}^-, X_{\rm H}^-) = 16$.

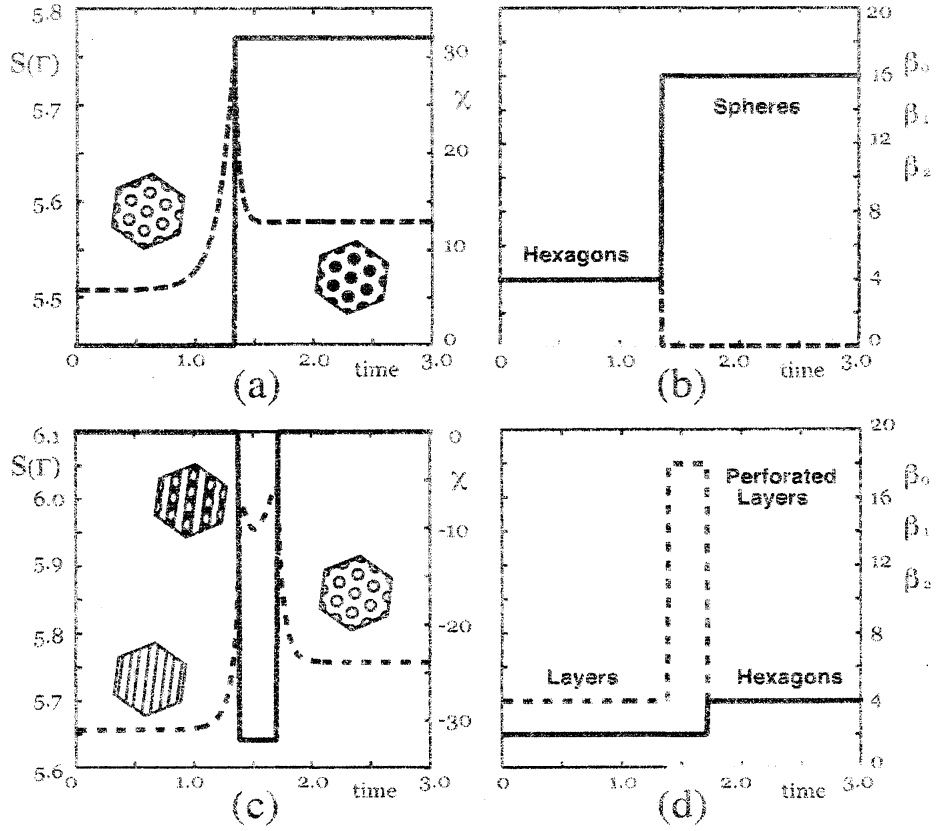

Figure 2: (a) Transition from hexagons to spheres for $(\overline{u}, \epsilon) = (0.30, 4.0 \times 10^{-2})$. left axis and gray line: surface area $S(\Gamma)$; right axis and solid line: Euler characteristic $\chi(\Gamma)$. (b) solid line: zeroth Betti number $\beta_0(X^-)$; broken line: first Betti number $\beta_1(X^-)$; gray line: second Betti number $\beta_2(X^-)$. (c,d) Transition from layers to hexagons for $(\overline{u}, \epsilon) = (0.20, 4.0 \times 10^{-2})$.

Considering cylindric domains placed in the diagonal direction of the periodic cube region, Ω, and assuming $u = -1$ inside the domain, we obtain an energy density, $\mathcal{F}_{\epsilon,\sigma}$, at the singular limit as follows:

$$\frac{\mathcal{F}_{\epsilon,\sigma}}{\epsilon} = \frac{2\sqrt{2}}{3}\frac{\sqrt{2\sqrt{3}\pi(1-\overline{u})}}{L} + \left(\frac{\sigma}{\epsilon}\right)\frac{(1-\overline{u})^2}{2\sqrt{3}}L^2(c(\overline{u}) + R(\zeta)). \tag{3}$$

Here the function $c(\overline{u})$ is defined by the fundamental solution of the Laplace operator; for $R(\zeta)$, see reference [3]. On the layers-hexagons phase boundary, the interval of hexagon alignment ($\sqrt{3}/2$ times the cylinder center-center distance) is almost equal to $2^{-3/2}$ times the laminar stripe interval. In this situation, the columnar domain can be placed inside the laminar domain in the $\langle 110 \rangle$ direction in two ways: the two diagonal directions of the rectangle. Therefore, when the laminar interface is destabilized, eight holes are created in the position on the mesh at the vertical angle, $\cos^{-1}(1/3) \approx 70.53°$, at which waves in two directions reinforce each other, i.e., perforated layers morphology is being formed as an intermediate state. Therefore, at

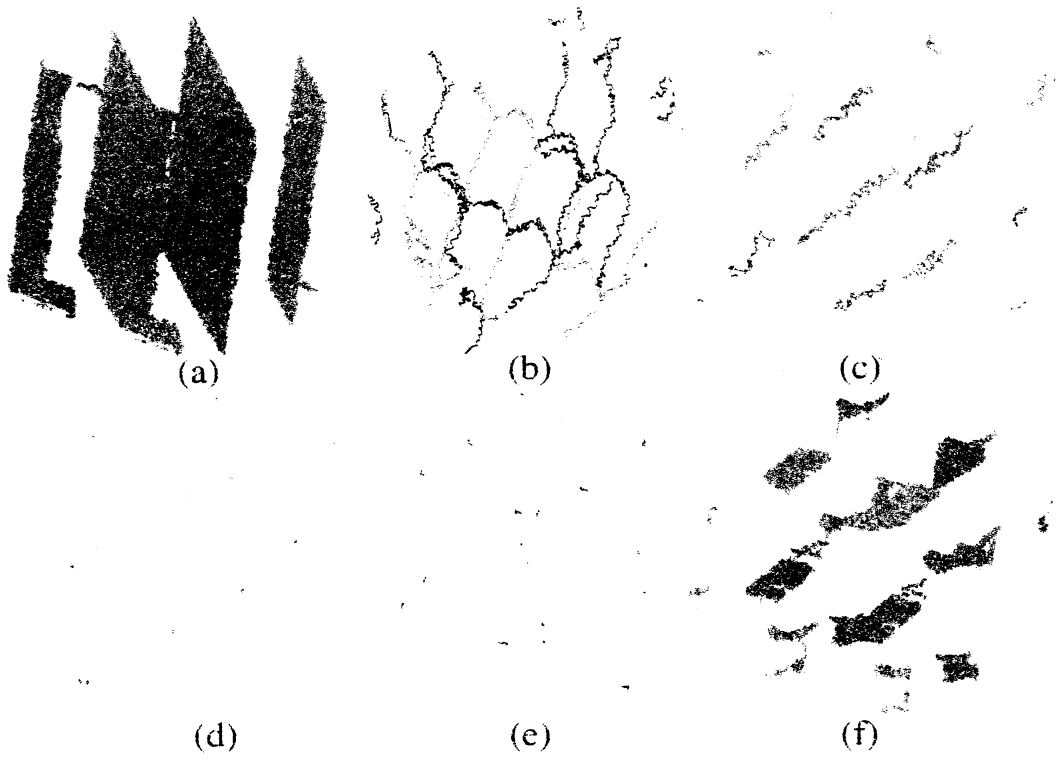

Figure 3: Abstract homology generators are shown in (a) Layers; (b) Perforated Layers; (c) Hexagons; (d) Layers relative to Perforated Layers; (e) Perforated Layers relative to Hexagons; (f) Layers relative to Hexagons with $\beta_2(X_{\mathrm{L}}^-, X_{\mathrm{H}}^-) = \beta_1(X_{\mathrm{L}}^-, X_{\mathrm{H}}^-) = 4$.

the first stage of transition from layers to hexagons, eight holes are created on each laminar domain and each perforated domain separates into two columnar domains at the next stage.

Finally, we show the abstract homology generators for the morphologies observed during the transition from layers to hexagons. As shown in Figs.3(a)-(c), the generators of layers are represented by two-dimensional elementary cubes and those of perforated layers and hexagons by one-dimensional ones. The homology generators are the basis elements for the Homology group H_k, that is, they are the chain complexes that generate H_k, and in this way they can be understood as combinations of elementary cubes. A more complete treatment can be found in the reference [4]. The relative cubical sets for $H_2(X_{\mathrm{L}}^-, X_{\mathrm{PL}}^-)$ and $H_1(X_{\mathrm{PL}}^-, X_{\mathrm{H}}^-)$ are also depicted in terms of related cubical sets in Figs.3(d)(e). It is worth nothing that if the k-th relative Betti numbers provide the number of k-dimensional critical events during morphology transition, a set of generators allows to locate them. At the first transition from layers to perforated layers, perforation holes are created so as to form a body-centered cubic structure. The relative homology generators at the subsequent transition show the same symmetry, in which the perforated layer domains split into columnar domains. Perforation (resp. splitting) can be regarded as the sign of a

stable (resp. unstable) manifold of perforated layer morphology.

We demonstrate specific applications of computational homology to characterize the morphology transition of the diblock copolymer problem. We apply these techniques as a measure of the complexity of numerically simulated three-dimensional morphologies like perforated layers, hexagons, spheres, etc. These structures arise as nodal domains of real-valued functions, for instance, concentration fields of two different components. The definitive identification of morphology transition is based on homological quantities, such as the Betti numbers and the relative homology group and its generators. Computational homology allows us to distinguish patterns at different parameter values, detect complicated spatio-temporal dynamics, compare experimental data with numerical simulations, among other things.

References

[1] Computational Homology Project, http://chomp.rutgers.edu.

[2] 計算ホモロジーとその応用 (応用数理サマーセミナー 2007, 日本応用数理学会・北海道大学数学 COE 共催), Hokkaido University Technical Report Series in Mathematics, No.124 (2007) [in Japanese].

[3] Chen, X., and Oshita Y., Applications of modular functions to interfacial dynamics, Arch. Rat. Mech. Anal. **186** (2007), 109-132.

[4] Kaczynski, T., Mischaikow, K., and Mrozek, M., Computational Homology, Springer-Verlag, NewYork (2004).

[5] Nishiura, Y., and Ohnishi, I., Some mathematical aspects of the micro-phase separation in diblock copolymers, Physica D **84**(1995), 31-39.

[6] Teramoto, T. and Nishiura, Y., *"Double Gyroid Morphology in a Gradient System with Nonlocal Effects"*, J. Phys. Soc. Jpn. **71** (2002), 1611-1614.

[7] Teramoto, T. and Nishiura, Y., *"Double Gyroid Morphology of Diblock Copolymer Problem"*, RIMS Kokyuroku No.1356 (2004), 116-121.